International Journal of Developmental Neuroscience 73 (2019) 83–88

Contents lists available at ScienceDirect

International Journal of Developmental Neuroscience

journal homepage: www.elsevier.com/locate/ijdevneu

Surface- and voxel-based brain morphologic study in Rett and Rett-like syndrome with *MECP2* mutation

Tadashi Shiohama[a,b,*], Jacob Levman[a,c], Emi Takahashi[a]

[a] Division of Newborn Medicine, Department of Medicine, Boston Children's Hospital, Harvard Medical School, 300 Longwood Avenue, Boston, MA, 02115, USA
[b] Department of Pediatrics, Chiba University Hospital, Inohana 1-8-1, Chiba-shi, Chiba, 2608670, Japan
[c] Department of Mathematics, Statistics and Computer Science, St. Francis Xavier University, 2323 Notre Dame Ave, Antigonish, Nova Scotia, B2G 2W5, Canada

ARTICLE INFO

Keywords:
Rett syndrome
MECP2
Structural brain MRI
Cerebellum

ABSTRACT

Rett syndrome (RTT) is a rare congenital disorder which in most cases (95%) is caused by methyl-CpG binding protein 2 (*MECP2*) mutations. RTT is characterized by regression in global development, epilepsy, autistic features, acquired microcephaly, habitual hand clapping, loss of purposeful hand skills, and autonomic dysfunctions. Although the literature has demonstrated decreased volumes of the cerebrum, cerebellum, and the caudate nucleus in RTT patients, surface-based brain morphology including cortical thickness and cortical gyrification analyses are lacking in RTT. We present quantitative surface- and voxel-based morphological measurements in young children with RTT and Rett-like syndrome (RTT-l) with *MECP2* mutations. The 8 structural T1-weighted MR images were obtained from 7 female patients with *MECP2* mutations (3 classic RTT, 2 variant RTT, and 2 RTT-l) (mean age 5.2 [standard deviation 3.3] years old). Our analyses demonstrated decreased total volumes of the cerebellum in RTT/RTT-l compared to gender- and age-matched controls ($t(22) = -2.93$, $p = .008$, Cohen's $d = 1.27$). In contrast, global cerebral cortical surface areas, global/regional cortical thicknesses, the degree of global gyrification, and global/regional gray and white matter volumes were not statistically significantly different between the two groups. Our findings, as well as literature findings, suggest that early brain abnormalities associated with RTT/RTT-l (with *MECP2* mutations) can be detected as regionally decreased cerebellar volumes. Decreased cerebellar volume may be helpful for understanding the etiology of RTT/RTT-l.

1. Introduction

Rett syndrome (RTT) (OMIM 312750) is a rare congenital disorder characterized by autistic features, acquired microcephaly, habitual hand clapping, loss of purposeful hand skill, and autonomic dysfunction (Neul et al., 2010; Singh and Santosh, 2018). Mutations of methyl-CpG binding protein 2 (*MECP2*) on the X chromosome are identified in over 90% of patients with a typical RTT phenotype. *MECP2* mutations were mainly identified in females with RTT and Rett-like syndrome (RTT-l), while males with MECP2 mutations mainly present with severe encephalopathy and fulfil the criteria of variant RTT as they develop (Neul et al., 2018; Soffer and Sidlow, 2016; Tokaji et al., 2018).

Typical RTT patients show normal development during infantile periods, followed by a severe decline in global development, decreased head circumference, and the emergence of epilepsy after 6–18 months (Neul et al., 2010; Krishnaraj et al., 2017; Hagberg et al., 2001; Dolce et al., 2013). This regression in RTT has motivated many research studies towards developing clinical interventions for RTT (as reviewed (Singh and Santosh, 2018)) and searching for biomarkers for early diagnosis of RTT using multiple techniques including neuroimaging.

Few studies have focused on quantitative brain morphology of RTT which has included 4 classical studies with manual trace-based measurements (Reiss et al., 1993; Casanova et al., 1991; Murakami et al., 1992; Subramaniam et al., 1997) as well as 1 study with voxel-based measurements (Carter et al., 2008). Although these studies showed decreased volumes of the cerebrum, cerebellum, and the caudate nucleus (Reiss et al., 1993; Carter et al., 2008), surface-based brain morphology including cortical gyrification and regional cortical thickness has not been explored. In this study, we report results from a quantitative brain morphological study with surface- and voxel-based

Abbreviations: RTT, Rett syndrome; RTT-l, Rett-like syndrome; NC, normal controls; GM, gray matter; WM, white matter; GI, gyrification index; RFT, Random field theory; FDR, false discovery rate

* Corresponding author at: Boston Children's Hospital, 300 Longwood Avenue, Boston, MA, 02115, USA.
E-mail address: asuha_hare@yahoo.co.jp (T. Shiohama).

https://doi.org/10.1016/j.ijdevneu.2019.01.005
Received 3 December 2018; Received in revised form 20 December 2018; Accepted 23 January 2019
Available online 25 January 2019

Table 1
The background of RTT and RTT-l participants.

Case number	1	2	3	4	5	6	7
Gender	Female	Female	Female	Female	Female	Female	Female
Age at diagnosis (years)	6.0	8.9	4.9	10.0	4.4	11.1	17.6
Age at MRI scan (years)	1.9	6.7	1.9	6.6	2.4	3.4, 7.3	11.1
Gestation period	Term	Term	Term	Term	Term	Term	Term
Clinical RTT type	Classic RTT	Variant RTT	Classic RTT	RTT-l	RTT-l	Variant RTT	Classic RTT
Main criteria for RTT diagnosis*	1,2,3,4	2,3	1,2,3,4	3,4	3,4	2,3,4	1,2,3,4
Supportive criteria for atypical RTT**	1,2,4,7,9	3,4,5,7,9	1,2,4,9	3,4,6,9	2,4,5,7	3,4,6,7,9	1,2,3,6,7,8
Autistic features	+	–	+	+	+	+	–
Epilepsy	+	+	–	–	+	+	+
Other clinical findings			Constipation	Constipation		Chiari malformation, GER	Prolonged QT interval, GER
Genetic test of *MECP2*	p.R168X	c.820_1193del	p.R306C	c.925C > Tp.R309W	p.P255R	C.1155_1172delCCTG	c.771_814del p.E258Gfs*58

Revised RTT criteria: 4 main criteria for classic RTT, and 2 main criteria and 5 supportive criteria at least for variant RTT were required (see the report by Neul et al. for detail criteria (Neul et al., 2010)).
Abbreviations; RTT, Rett syndrome; RTT-l, Rett-like syndrome; GER, Gastroesophageal reflux.
* Main criteria: 1. loss of acquired purposeful hand skills; 2. loss of acquired spoken language; 3. gait abnormalities; 4. stereotypic hand movements.
** Supportive criteria: 1. breathing disturbances when awake; 2. bruxism when awake; 3. impaired sleep pattern; 4. abnormal muscle tone; 5. peripheral vasomotor disturbances; 6. scoliosis/kyphosis; 7. growth retardation; 8. small cold hands and feet; 9. Inappropriate laughing/screaming spells; 10. diminished response to pain; 11. Intense eye communication.

measurements in young children with RTT/RTT-l.

2. Patients and methods

2.1. Patients

The Institutional Review Board at Boston Children Hospital (BCH) approved this retrospective study. We assembled our listing of RTT susceptive patients using i2b2 (http://web2.tch.harvard.edu/i2b2). Based on clinical records at BCH, clinical diagnosis by a pediatric neurologist was confirmed using revised RTT diagnostic criteria (Neul et al., 2010). As shown in Tables 1 and 3 patients fulfilled the classic RTT criteria, and 2 patients fulfilled the variant RTT criteria. The other 2 patients were RTT-l; although 2 main criteria were fulfilled, only 4 supportive criteria were fulfilled (one more supportive criterion is necessary to critically diagnose as RTT). We obtained 8 MRI data sets and electronic medical records from those 7 cases of RTT/RTT-l. We obtained 8 MRI data sets and electronic medical records from those 7 cases of RTT/RTT-l. The 16 gender- and age-matched normal controls (NC) were selected from our in-house database composed of electronic records of healthy participants without neurological disorders, neuropsychological disorders or epilepsy (Levman et al., 2017). Both datasets (RTT/RTT-l and NC) were comprised of examination acquired at BCH on the same suite of MRI scanners.

2.2. Structural MRI acquisition and processing

Three-dimensional (3-D) T1-weighted MPRAGE images (TR 2000–2500 ms; TE 1.7–2.5 ms, voxel size 0.85–1 × 0.85–1 x 1 mm, matrix 256 × 256) were obtained from all participants included in this study with clinical 3 T MRI scanners (MAGNETOM Skyra, Siemens Medical Systems, Erlangen, Germany). DICOM files were collected through the Children's Research and Integration System (Pienaar et al., 2015), and analyzed with CIVET version 2.1.0 pipeline (Zijdenbos et al., 2002) on the CBRAIN platform (Sherif et al., 2014). Corrections for non-uniform intensity artifacts by the N3 algorithm (Sled et al., 1998), stereotaxic registration (onto the icbm152 non-linear 2009 template) (Fonov et al., 2009), and brain masking (Smith, 2002) were performed. A voxel-based volumetric analysis was performed with tissue classification using an artificial neural network classifier (INSECT) (Tohka et al., 2004), and segmentation of brain regions was performed with ANIMAL (Collins et al., 1999). For a surface-based analysis, the surfaces of the gray matter and white matter were extracted by using 40,962 vertices per hemisphere with the t-laplace metric (Kim et al., 2005; Boucher et al., 2009), and cortical surface parameters including the gyrification index (GI), average cortex thickness, cortical surface area, and cortical volumes were calculated in each hemisphere.

The quality of the outputs of the CIVET pipeline (shapes of the brain mask, linear/non-linear registration to the template, tissue classification, and brain segmentation) were manually inspected for quality. This resulted in 8 volumetric structural brain MR images from 7 RTT/RTT-l patients with *MECP2* mutations.

2.3. Statistical analyses

Each brain structural measurement in RTT/RTT-l and NC participants were evaluated through Levene's test for equality of variances and two-tailed unpaired *t*-test for equality of means. According to the false discovery rate correction for multiple comparisons by the Benjamini-Hochberg procedure (Benjamini et al., 2001; Reiner et al., 2003), Benjamini-Hochberg critical values ($\alpha = .05$, $q = .25$) were determined for 57 and 40 repeating *t*-tests in surface- and voxel-based measurements, respectively. IBM SPSS Statistics version 19 (IBM Corp. Armonk, NY) was used for the statistical analysis. Regional cortical thickness was statistically analyzed and visualized as t-statistic maps, random field theory (RFT) maps, and false discovery rate (FDR) maps using the SurfStat toolbox (http://www.math.mcgill.ca/keith/surfstat/) with MATLAB R2016a (MathWorks, Natick, MA).

3. Results

3.1. Participants' background

Clinical information for the 7 RTT/RTT-l participants are shown in Table 1. All participants were females, and born at term gestation. Age at MRI scans were not statistically significantly different ($T(22) = -.011$, $P = .991$) between RTT/RTT-l ($N = 8$) and NC ($N = 16$) based on Student's *t*-test (the mean [standard deviation] were 5.2 [3.3] and 5.2 [3.2] years old in RTT/RTT-l and NC participants, respectively). Qualitative analyses of brain MRI showed no abnormal parenchymal findings in both RTT/RTT-l and NC participants, except for high signal intensity in T2-weighted images in the right cerebellar hemisphere in case 7.

3.2. Voxel-based volumetric analysis

Global and regional volumes in the cerebrum showed no statistically

Table 2
The brain volume of RTT/RTT-l and NC participants.

	RTT/RTT-l (N = 8) Mean [SD]	NC (N = 16) Mean [SD]	The rate of RTT/RTT-l to NC	Absolute Cohen's *d*	*P* value
CSF (mm^3)	30686 [13467]	26277 [12155]	1.17	0.35	.43
Cortical GM (mm^3)	526269 [103942]	546403 [69438]	0.96	0.25	.58
WM (mm^3)	315219 [33612]	340810 [60879]	0.92	0.48	.20
Subcortical GM (mm^3)	31862 [7519]	35717 [4146]	0.89	0.71	.21

Abbreviation; RTT, Rett syndrome; RTT-l, Rett-like syndrome; NC, Normal controls; SD, Standard deviation; CSF, Cerebrospinal fluid; GM, Gray matter; WM, White matter.

Table 3
The brain segmental volumes of RTT/RTT-l and NC participants.

Measurement (ANIMAL segmentation number)	RTT/RTT-l (N = 8) Mean [SD] (mm^3)	NC (N = 16) Mean [SD] (mm^3)	The rate of RTT/RTT-l to NC	Absolute Cohen's *d*	*P* value
L frontal GM (210)	130215 [29180]	142544 [13812]	0.91	0.62	.29
R frontal GM (211)	131702 [30415]	142803 [13332]	0.92	0.54	.35
L frontal WM (30)	65786 [9853]	71538 [12195]	0.92	0.5	.26
R frontal WM (17)	6649 [9529]	71215 [12066]	0.93	0.42	.35
L temporal GM (218)	88195 [19237]	94798 [11449]	0.93	0.46	.30
R temporal GM (219)	90617 [17693]	96589 [10499]	0.94	0.45	.31
R temporal WM (59)	33712 [5265]	37041 [7251]	0.91	0.5	.26
L temporal WM (83)	33571 [5338]	37283 [7042]	0.90	0.57	.20
L parietal GM (6)	71589 [21420]	76793 [7423]	0.93	0.38	.52
R parietal GM (2)	70708 [17865]	76737 [7366]	0.92	0.51	.39
L parietal WM (57)	36109 [5618]	40262 [8003]	0.90	0.57	.20
R parietal WM (105)	35004 [4127]	39973 [8136]	0.88	0.7	.12
L occipital GM (8)	37000 [8130]	38847 [5260]	0.95	0.29	.51
R occipital GM (4)	38783 [9857]	40040 [5415]	0.97	0.18	.69
L occipital WM (73)	16365 [1911]	18199 [3008]	0.90	0.68	.13
R occipital WM (45)	16184 [2010]	18017 [3847]	0.90	0.54	.14
L thalamus (102)	6148 [664]	6663 [686]	0.92	0.76	.094
R thalamus (203)	6197 [598]	6671 [635]	0.93	0.76	.093
L caudate (39)	3886 [733.5]	4413 [600.5]	0.88	0.82	.073
R caudate (53)	3864 [556]	4381 [536]	0.88	0.95	.039
L fornix (29)	518 [108]	541 [81]	0.96	0.26	.55
R fornix (254)	500 [93]	516 [74]	0.97	0.2	.65
L globus pallidus (12)	943 [184]	1014 [128]	0.93	0.48	.28
R globus pallidus (11)	936 [164]	983 [129]	0.95	0.33	.45
L putamen (14)	3665 [624]	4129 [506]	0.89	0.85	.063
R putamen (16)	3746 [582]	4222 [534]	0.89	0.87	.058
L subthalamic nucleus (33)	39.0 [7.3]	43.4 [5.6]	0.90	0.72	.11
R subthalamic nucleus (23)	39.3 [8.2]	44.7 [5.4]	0.88	0.85	.12
Brainstem (20)	21991 [3426]	24655 [3822]	0.89	0.72	.11
L cerebellum (67)*	56844 [7801]	67107 [7908]	0.85	1.3	.0064
R cerebellum (76)*	57299 [7127]	66309 [7523]	0.86	1.22	.010
L lateral ventricle (3)	3582 [2543]	3102 [1146]	1.15	0.28	.62
R lateral ventricle (9)	2892 [1980]	2900 [1288]	1.00	0.01	.99
3rd ventricle (232)	1419 [750]	1308 [487]	1.10	0.19	.67
4th ventricle (233)	1304 [376]	1814 [794]	0.72	0.74	.10
Extracerebral CSF (255)	340219 [62244]	284400 [85115]	1.20	0.71	.12

Abbreviation; RTT, Rett syndrome; RTT-l, Rett-like syndrome; NC, Normal controls; SD, Standard deviation; L, left; R, right; GM, gray matter; WM, white matter; CSF, cerebrospinal fluid; * $p < .0125$ (two-tailed unpaired *t* test with false discovery rate correction).

significant difference between RTT/RTT-l and NC participants (Tables 2 and 3), while bilateral cerebellar hemispheres demonstrated statistically significantly decreased volumes in RTT/RTT-l compared to those in NC (the rate of RTT/RTT-l to NT = 0.85, 0.86, and 0.86, absolute Cohen's $d = 1.3$, 1.22, and 1.27, and $p = .0064$, .010, and .008 in left, right, and total cerebellum, respectively). Scatter plots (volume vs. age) showed that the decrease in cerebellar volume was not age-dependent but rather case-dependent (Fig. 2). Genotype-phenotype correlation (correlation between mutation diversities and total cerebellar volumes) was not seen between RTT/RTT-l patients with intact or aberrant cerebellar volume.

3.3. Surface-based cortical analysis

The surface-based analyses showed that in the cerebrum, the surface area, thickness, volume, and GI were not statistically significantly different between RTT/RTT-l and NC participants (Tables 4 and 5). Fig. 1 shows a cortical thickness map superimposed on a 3-D template brain surface. The t-tests showed increased thickness in the right insula, and decreased thickness in the left precentral gyrus and left cuneus in RTT/RTT-l (Fig. 1). After the correction for multiple comparisons with RFT ($p < .02$) and FDR ($p < .05$), there was no region that showed statistically significantly different thickness in the cortex between RTT/RTT-l and NC.

4. Discussion

We analyzed surface- and voxel-based measurements in structural brain MRI of patients with RTT. The global cortical gyrification, thickness, and volume (Tables 2 and 3), as well as regional cortical thickness (Fig.1) in surface-based analysis, and the regional volumes of the cerebrum (Table 4) in voxel-based analysis showed no statistically significant difference between RTT/RTT-l and NC participants. The volumes of bilateral cerebellar hemispheres (Table 3) were significantly

Table 4
The surface based cortical measurements in RTT/RTT-l and NC participants.

	RTT/RTT-l (N = 8) Mean [SD]	NC (N = 16) Mean [SD]	The rate of RTT/RTT-l to NC	Absolute Cohen's *d*	*P* value
Gyrification Index	3.71 [0.28]	3.78 [0.14]	0.98	0.36	.41
L gyrification index	2.71 [0.20]	2.76 [0.10]	0.98	0.38	.39
R gyrification index	2.71 [0.19]	2.79 [0.11]	0.97	0.55	.21
L cortex surface area (mm^2)	87420 [12932]	91680 [8844]	0.95	0.41	.35
R cortex surface area (mm^2)	87442 [12319]	92588 [8353]	0.94	0.53	.24
L cortex average thickness (mm)	2.86 [0.35]	2.73 [0.30]	1.04	0.38	.38
R cortex average thickness (mm)	2.88 [0.38]	2.74 [0.288]	1.05	0.42	.34
L cortex volume (mm^3)	240211 [41297]	245002 [37804]	0.98	0.12	.78
R cortex volume (mm^3)	240722 [33831]	247545 [36334]	0.97	0.19	.66

Abbreviation; RTT, Rett syndrome; RTT-l, Rett-like syndrome; NC, Normal controls; SD, standard deviation; L, left hemisphere; R, right hemisphere.

Table 5
The *p* value in compartments of surface based cortical measurements between RTT/RTT-l and NC participants.

	Surface area	Cortical thickness	Cortical volume	Gyrification index
Hemisphere, left	.35	.38	.78	.39
Hemisphere, right	.24	.34	.66	.21
Parietal lobe, left	.16	.43	.37	N.A.
Parietal lobe, right	.18	.38	.41	N.A.
Occipital lobe, left	.74	.90	.84	N.A.
Occipital lobe, right	.49	.78	.67	N.A.
Frontal lobe, left	.49	.40	.95	N.A.
Frontal lobe, right	.24	.38	.67	N.A.
Isthmus lobe, left	.91	.32	.49	N.A.
Isthmus lobe, right	.99	.36	.52	N.A.
Parahippocampal lobe, left	.031	.22	.56	N.A.
Parahippocampal lobe, right	.082	.27	.70	N.A.
Cingulate lobe, left	.44	.17	.69	N.A.
Cingulate lobe, right	.88	.18	.41	N.A.
Temporal lobe, left	.43	.46	.83	N.A.
Temporal lobe, right	.30	.42	.71	N.A.
Insula lobe, left	.14	.096	.76	N.A.
Insula lobe, right	.099	.074	.68	N.A.

Abbreviation; RTT, Rett syndrome; RTT-l, Rett-like syndrome; NC, normal controls; N.A., not acquired.

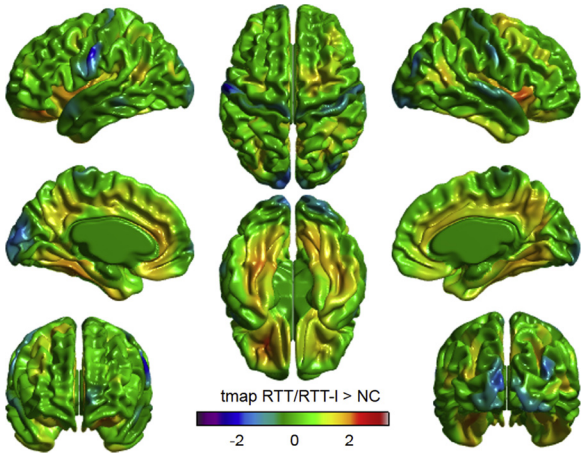

Fig. 1. Visualized cortical thickness with t statistics map showing thicker lesions in Rett and Rett-like syndrome (RTT/RTT-l, N = 8) than normal controls (NC, N = 16). In the color scale, blue and red indicate less and greater in mean cortical thickness in RTT/RTT-l, respectively, compared to NC (For interpretation of the references to colour in this figure legend, the reader is referred to the web version of this article).

decreased in RTT/RTT-l compared to those in NC.

Although acquired microcephaly is an essential clinical manifestation in RTT, only some studies have reported results of quantitative analyses of structural brain MRI in RTT (Reiss et al., 1993; Casanova et al., 1991; Murakami et al., 1992; Subramaniam et al., 1997; Carter et al., 2008). Previous studies reported decreased volumes in the cerebrum (Reiss et al., 1993; Casanova et al., 1991; Murakami et al., 1992; Subramaniam et al., 1997; Carter et al., 2008), basal ganglia (Reiss et al., 1993; Casanova et al., 1991; Murakami et al., 1992), cerebellum (Casanova et al., 1991; Murakami et al., 1992), corpus callosum (Murakami et al., 1992), and brainstem (Reiss et al., 1993; Murakami et al., 1992) in RTT compared to those in NC. The volume reduction of the cerebrum and the cerebellum have been confirmed in brain MRI studies with a mecp2 hetero- or homozygous-knockout mouse model (Ward et al., 2008; Allemang-Grand et al., 2017; Saywell et al., 2006).

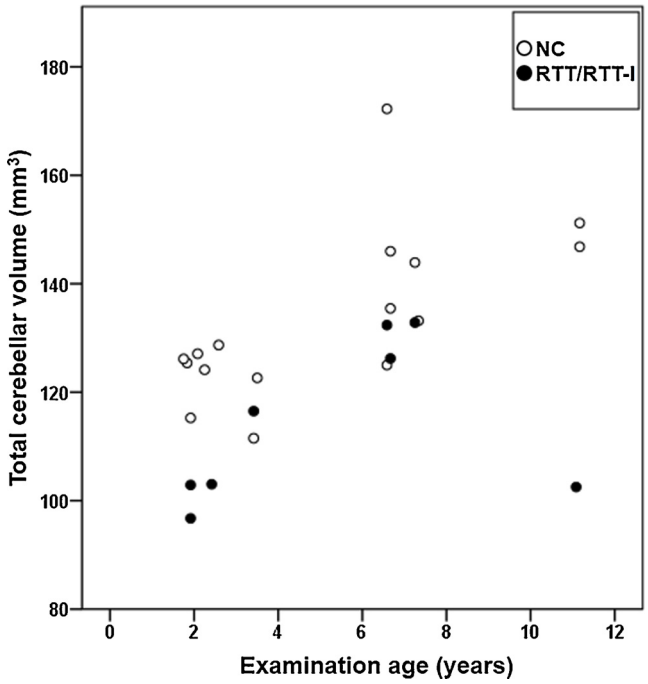

Fig. 2. Scatter plots (age vs. volume) of total cerebellar volume. Closed circles and open circles indicate Rett and Rett-like syndrome (RTT/RTT-l, N = 8) and normal controls (NC, N = 16), respectively.

However, in our study, a statistically significant difference between RTT/RTT-l and NC was observed only in the cerebellar volume. Given that the RTT/RTT-l patients in our study were younger than the prior studies (mean age: 5.2 years old, compared to 5.3–12 years old in the past studies) (Reiss et al., 1993; Casanova et al., 1991; Murakami et al., 1992; Subramaniam et al., 1997; Carter et al., 2008), it is possible to interpret our results to suggest that the cerebellar volume loss precedes atrophy of other brain regions, which potentially can contribute to an early diagnosis of RTT/RTT-l.

It is reasonable for the loss of cerebellar volumes to be associated with RTT, because RTT patients and mouse models present cerebellar symptoms; e.g. truncal ataxia (Diagnostic criteria for Rett syndrome, 1988; Temudo et al., 2008) and tremor (Temudo et al., 2008) in RTT patients and, tremor (Chen et al., 2001; Guy et al., 2001) and ataxic gaze (Gadalla et al., 2014) in *mecp2*-deficient mice. Postmortem examinations of the cerebellum of five RTT females ranging in age from 7 to 30 years revealed a loss of Purkinje cells, atrophy and gliosis (Oldfors et al., 1990). In heterozygous *mecp2*-deficient mice, the cell bodies of cerebellar granule neurons are smaller and more densely packed than those in the wild type (Chen et al., 2001).

The MECP2 protein, encoded by *MECP2*, is a chromatin-associated protein, which binds to methylated DNA and modifies transcription (Lyst and Bird, 2015). In humans, *MECP2* expression increases after birth and maintains high expression levels in mature neurons and glial cells of the cerebrum and in molecular layers of the cerebellum (Armstrong et al., 1995). In the cerebrum, MECP2 maintains normal function of mature neurons (Lyst and Bird, 2015; Cheval et al., 2012; McGraw et al., 2011; Nguyen et al., 2012) and morphology of neural dendrites (Ballas et al., 2009), but does not regulate neuronal morphology (Lyst and Bird, 2015). Given that the cerebellum develops until the first postnatal years in humans, unlike the cerebrum (Ten Donkelaar and Lammens, 2009), *MECP2* expression in postnatal periods likely contributes to cerebellar development (Armstrong et al., 1995; Mullaney et al., 2004; Liu et al., 2017) along with a maintenance role in the cerebrum. The literature and our current findings that regional decreased volume was observed only in the cerebellum in patients with RTT/RTT-l together suggest that early brain abnormalities likely caused by *MECP2* in patients with RTT/RTT-l can be detectable as decreased volumes of the cerebellar hemispheres with structural MRI.

5. Conclusion

We analyzed structural brain MRI examinations of children with RTT/RTT-l by surface- and voxel-based measurements, and found statistically significantly decreased volumes of the cerebellum in RTT/RTT-l compared to those in normal controls. In contrast, cerebral cortical area, thickness, volumes, and gyrification, as well as subcortical gray matter volumes were not statistically significant between the two groups. The decreased cerebellar volume may be helpful for understanding the etiology of RTT/RTT-l.

Author contributions

T.S. was responsible for study design. T.S., and J.L. analyzed data, and T.S., J.L., and E.T. wrote/edited the manuscript.

Conflict of interest

T.S., J. L., and E. T. declare relevant no conflicts of interest.

Study funding

This research project was supported by NIHR01HD078561, R21MH118739, and R03NS101372to E.T.

Ethical approval

All procedures performed in studies involving human participants were in accordance with the ethical standards of the institutional and/or national research committee and with the 1964 Helsinki declaration and its later amendments or comparable ethical standards. For this type of study formal consent is not required.

Acknowledge

We would like to thank Patrick MacDonald and Ashley Ruyan Lim at Boston Children's Hospital for technical support.

References

Allemang-Grand, R., Ellegood, J., Spencer Noakes, L., et al., 2017. Neuroanatomy in mouse models of Rett syndrome is related to the severity of Mecp2 mutation and behavioral phenotypes. Mol. Autism 8, 32.
Armstrong, D., Dunn, J.K., Antalffy, B., Trivedi, R., 1995. Selective dendritic alterations in the cortex of Rett syndrome. J. Neuropathol. Exp. Neurol. 54, 195–201.
Ballas, N., Lioy, D.T., Grunseich, C., Mandel, G., 2009. Non-cell autonomous influence of MeCP2-deficient glia on neuronal dendritic morphology. Nat. Neurosci. 12, 311–317.
Benjamini, Y., Drai, D., Elmer, G., Kafkafi, N., Golani, I., 2001. Controlling the false discovery rate in behavior genetics research. Behav. Brain Res. 125, 279–284.
Boucher, M., Whitesides, S., Evans, A., 2009. Depth potential function for folding pattern representation, registration, and analysis. Med. Image Anal. 13, 203–214.
Carter, J.C., Lanham, D.C., Pham, D., Bibat, G., Naidu, S., Kaufmann, W.E., 2008. Selective cerebral volume reduction in Rett syndrome: a multiple-approach MR imaging study. AJNR Am. J. Neuroradiol. 29, 436–441.
Casanova, M.F., Naidu, S., Goldberg, T.E., et al., 1991. Quantitative magnetic resonance imaging in Rett syndrome. J. Neuropsychiatry Clin. Neurosci. 3, 66–72.
Chen, R.Z., Akbarian, S., Tudor, M., Jaenisch, R., 2001. Deficiency of methyl-CpG binding protein-2 in CNS neurons results in a Rett-like phenotype in mice. Nat. Genet. 27, 327–331.
Cheval, H., Guy, J., Merusi, C., De Sousa, D., Selfridge, J., Bird, A., 2012. Postnatal inactivation reveals enhanced requirement for MeCP2 at distinct age windows. Hum. Mol. Genet. 21, 3806–3814.
Collins, D.L., Zijdenbos, A.P., Baaré, W.F.C., Evans, A.C., 1999. ANIMAL + INSECT: improved cortical structure segmentation. In: In: Kuba, A., Šáamal, M., Todd-Pokropek, A. (Eds.), Information Processing in Medical Imaging. Lecture Notes in Computer Science 1613. Springer, Berlin, Heidelberg, pp. 210–223.
Diagnostic criteria for Rett syndrome, 1988. The rett syndrome diagnostic criteria work group. Ann. Neurol. 23, 425–428.
Dolce, A., Ben-Zeev, B., Naidu, S., Kossoff, E.H., 2013. Rett syndrome and epilepsy: an update for child neurologists. Pediatr. Neurol. 48, 337–345.
Fonov, V.S., Evans, A.C., McKinstry, R.C., Almli, C.R., Collins, D.L.L., 2009. Unbiased nonlinear average age-appropriate brain templates from birth to adulthood. NeuroImage 47, S102. http://www.sciencedirect.com/science/article/pii/S1053811909708845.
Gadalla, K.K., Ross, P.D., Riddell, J.S., Bailey, M.E., Cobb, S.R., 2014. Gait analysis in a Mecp2 knockout mouse model of Rett syndrome reveals early-onset and progressive motor deficits. PLoS One 9, e112889.
Guy, J., Hendrich, B., Holmes, M., Martin, J.E., Bird, A., 2001. A mouse Mecp2-null mutation causes neurological symptoms that mimic Rett syndrome. Nat. Genet. 27, 322–326.
Hagberg, G., Stenbom, Y., Engerström, I.W., 2001. Head growth in Rett syndrome. Brain Dev. 23, S227–S229.
Kim, J.S., Singh, V., Lee, J.K., et al., 2005. Automated 3-D extraction and evaluation of the inner and outer cortical surfaces using a Laplacian map and partial volume effect classification. Neuroimage 27, 210–221.
Krishnaraj, R., Ho, G., Christodoulou, J., 2017. RettBASE: Rett syndrome database update. Hum. Mutat. 38, 922–931.
Levman, J., MacDonald, P., Lim, A.R., Forgeron, C., Takahashi, E., 2017. A pediatric structural MRI analysis of healthy brain development from newborns to young adults. Hum. Brain Mapp. 38, 5931–5942.
Liu, F., Ni, J.J., Sun, F.Y., 2017. Expression of phospho-MeCP2s in the developing rat brain and function of postnatal MeCP2 in cerebellar neural cell development. Neurosci. Bull. 33, 1–16.
Lyst, M.J., Bird, A., 2015. Rett syndrome: a complex disorder with simple roots. Nat. Rev. Genet. 16, 261–275.
McGraw, C.M., Samaco, R.C., Zoghbi, H.Y., 2011. Adult neural function requires MeCP2. Science 333, 186.
Mullaney, B.C., Johnston, M.V., Blue, M.E., 2004. Developmental expression of methyl-CpG binding protein 2 is dynamically regulated in the rodent brain. Neuroscience 123, 939–949.
Murakami, J.W., Courchesne, E., Haas, R.H., Press, G.A., Yeung-Courchesne, R., 1992. Cerebellar and cerebral abnormalities in Rett syndrome: a quantitative MR analysis. AJR Am. J. Roentgenol. 159, 177–183.
Neul, J.L., Kaufmann, W.E., Glaze, D.G., et al., 2010. Rett syndrome: revised diagnostic criteria and nomenclature. Ann. Neurol. 68, 944–950.
Neul, J.L., Benke, T.A., Marsh, E.D., et al., 2018. The array of clinical phenotypes of males with mutations in Methyl-CpG binding protein 2. Am. J. Med. Genet. B Neuropsychiatr. Genet.(December). https://doi.org/10.1002/ajmg.b.32707. [Epub ahead of print].
Nguyen, M.V., Du, F., Felice, C.A., et al., 2012. MeCP2 is critical for maintaining mature neuronal networks and global brain anatomy during late stages of postnatal brain development and in the mature adult brain. J. Neurosci. 32, 10021–10034.
Oldfors, A., Sourander, P., Armstrong, D.L., Percy, A.K., Witt-Engerström, I., Hagberg, B.A., 1990. Rett syndrome: cerebellar pathology. Pediatr. Neurol. 6, 310–314.
Pienaar, R., Rannou, N., Bernal, J., Hahn, D., Grant, P.E., 2015. ChRIS–A web-based neuroimaging and informatics system for collecting, organizing, processing, visualizing and sharing of medical data. Conf. Proc. IEEE Eng. Med. Biol. Soc. 2015,

206–209.
Reiner, A., Yekutieli, D., Benjamini, Y., 2003. Identifying differentially expressed genes using false discovery rate controlling procedures. Bioinformatics 19, 368–375.
Reiss, A.L., Faruque, F., Naidu, S., Abrams, M., Beaty, T., Bryan, R.N., Moser, H., 1993. Neuroanatomy of Rett syndrome: a volumetric imaging study. Ann. Neurol. 34, 227–234.
Saywell, V., Viola, A., Confort-Gouny, S., Le Fur, Y., Villard, L., Cozzone, P.J., 2006. Brain magnetic resonance study of Mecp2 deletion effects on anatomy and metabolism. Biochem. Biophys. Res. Commun. 340, 776–783.
Sherif, T., Rioux, P., Rousseau, M.E., et al., 2014. CBRAIN: a web-based, distributed computing platform for collaborative neuroimaging research. Front. Neuroinform. 8, 54.
Singh, J., Santosh, P., 2018. Key issues in Rett syndrome: emotional, behavioural and autonomic dysregulation (EBAD) - a target for clinical trials. Orphanet J. Rare Dis. 13, 128.
Sled, J.G., Zijdenbos, A.P., Evans, A.C., 1998. A nonparametric method for automatic correction of intensity nonuniformity in MRI data. IEEE Trans. Med. Imaging 17, 87–97.
Smith, S.M., 2002. Fast robust automated brain extraction. Hum. Brain Mapp. 17, 143–155.
Soffer, O.D., Sidlow, R., 2016. A rare MeCP2_e1 mutation first described in a male patient with severe neonatal encephalopathy. Am. J. Med. Genet. A 170, 1881–1883.
Subramaniam, B., Naidu, S., Reiss, A.L., 1997. Neuroanatomy in Rett syndrome: cerebral cortex and posterior fossa. Neurology 48, 399–407.
Temudo, T., Ramos, E., Dias, K., et al., 2008. Movement disorders in Rett syndrome: an analysis of 60 patients with detected MECP2 mutation and correlation with mutation type. Mov. Disord. 23, 1384–1390.
Ten Donkelaar, H.J., Lammens, M., 2009. Development of the human cerebellum and its disorders. Clin. Perinatol. 36, 513–530.
Tohka, J., Zijdenbos, A., Evans, A., 2004. Fast and robust parameter estimation for statistical partial volume models in brain MRI. Neuroimage 23, 84–97.
Tokaji, N., Ito, H., Kohmoto, T., et al., 2018. A rare male patient with classic Rett syndrome caused by MeCP2_e1 mutation. Am. J. Med. Genet. A 176, 699–702.
Ward, B.C., Agarwal, S., Wang, K., Berger-Sweeney, J., Kolodny, N.H., 2008. Longitudinal brain MRI study in a mouse model of Rett Syndrome and the effects of choline. Neurobiol. Dis. 31, 110–119.
Zijdenbos, A.P., Forghani, R., Evans, A.C., 2002. Automatic ""pipeline"" analysis of 3-D MRI data for clinical trials: application to multiple sclerosis. IEEE Trans. Med. Imaging 21, 1280–1291.